JOURNAL OF PROPULSION AND POWER
Vol. 24, No. 6, November–December 2008

Characterization of an Acoustically Self-Excited Combustor for Spray Evaporation

R. Balachandran,* S. R. Chakravarthy,† and R. I. Sujith
Indian Institute of Technology, Madras, Chennai 600 036, India

DOI: 10.2514/1.28851

A combustor with a divergent inlet passage and a coaxially movable bluff-body flame holder has been developed to enable self-excitation of high-amplitude acoustic oscillations, for the purpose of enhancing the rate of evaporation of water sprays. Commercially available liquid petroleum gas is used as fuel. The acoustic pressure levels and modal contents are controlled by varying the location of the bluff body along the axis of the combustor relative to its inlet. Locating the bluff body closer to the inlet yields higher acoustic pressure amplitudes over a wider range of fuel–air ratios. The excitation of high amplitudes is accompanied by a shift from the fundamental to the first harmonic at different fuel–air ratios for different air mass flow rates in the fuel-lean range. When high sound pressure levels are excited in the combustor, the heat transfer due to water cooling of the combustor walls and across the walls of the tailpipe increase considerably, up to 40% for an increase in sound pressure levels from 145 to 160 dB. Water-spray evaporation experiments are performed with low and high sound pressure levels of acoustic excitation for different water injection rates over a range of mass flow rates of fuel and air. For a given mass flow rate of air and fuel, it is found that the water evaporation rate increases significantly above a certain threshold acoustic pressure, up to 107% for a sound pressure level of 156 dB, despite the considerable increase in heat loss due to the acoustic oscillations.

I. Introduction

THE importance of improving the performance of devices involving energy-intensive processes such as spray drying and calcination, cannot be overstated. In such processes, the rate-controlling mechanisms are the heat and mass transfer between the gas phase and the droplets/particles in the condensed phase. If these rates can be increased by the of acoustic oscillations, the time required, for instance, to dry a typical droplet would decrease. This, in turn, would lead to increased productivity and savings in fuel costs. The reduced drying time would reduce the required size of a new dryer, which would also lead to savings in capital investment costs.

The possibility of using sound to increase the convective heat and mass transfer rates has received attention in recent times (e.g.,[1]). The goal of the present work is to develop a combustor that is capable of self-excitation of strong acoustic oscillations, which could be used to enhance the rate of liquid-spray evaporation. The self-excitation of acoustic oscillations is achieved in the present work by means of resonance with fluid-dynamic instabilities, including periodic vortex shedding from a bluff body in the combustion zone, resulting in oscillatory heat release. Schadow and Gutmark [2] reviewed the research related to the driving mechanism of dump combustor instability, with gaseous fuels. They summarized that vortex shedding is an important driving mechanism, and the development of coherent flow structures and their breakdown into fine-scale turbulence can lead to periodic heat release, which, when in phase with the pressure oscillations, can drive the latter, as stated by the Rayleigh criterion [3]. Gutmark et al. [4] investigated the interaction between fluid-dynamic and acoustic instabilities in combusting flows within ducts. Their results showed substantial increases in the amplitude of the instability when the fluid-dynamic frequency associated with large-scale coherent structures in the near field of the duct matched the acoustic mode frequency of the confining duct. Lieuwen et al. [5] point out that the convective and chemical heat-release time scales of the fuel–air mixture within the combustor may match the acoustic time scales for excitation of strong acoustic oscillations, and this could be amplified by equivalence-ratio fluctuations due to the response of the fuel feed line to the acoustic oscillations present in the combustion chamber. The vortex shedding at a location such as the dump plane in a dump combustor, for instance, would carry the fuel–air mixture in packets and modulate the heat-release fluctuations.

The effect of a strong acoustic field on the rate of evaporation of a liquid droplet was numerically investigated by Gemmen et al. [6]. They found that the evaporation rate of a 100 μm-sized droplet was increased by at least 160% for a sound pressure level of 174 dB over steady flow at the same mean Reynolds number. Sujith et al. [7] experimentally demonstrated the enhancement of the evaporation rate of ethanol and water droplets up to 100% in the presence of an externally imposed acoustic field at 160 dB. Their theoretical analysis showed that, as the acoustic velocity increased, the evaporation rate decreased until it reached a minimum and then increased significantly [8].

As opposed to the previous studies on single droplets, McQuay and Dubey [9] investigated the effect of the different harmonics of acoustic oscillations of 150 dB amplitude at 54, 106, and 162 Hz set up in a Rijke tube on the evaporation characteristics of a nonreacting ethanol spray using a phase Doppler particle size analyzer (PDPA). With the first and third acoustic natural modes excited in the tube, they found that the droplet diameters decreased by about 13–30% on the average. Note that because evaporation is a surface phenomenon, its rate is proportional to the square of the droplet diameter. The second mode had little effect on the droplet diameters because the location of the spray nozzle corresponded to a velocity node. Spectral analysis of the droplet's axial velocity component revealed dominant frequencies of the acoustic waves. The effect of an acoustic field of 150 dB amplitude at 80 Hz on an ethanol spray flame in a propane-fired Rijke tube pulse combustor was investigated by Dubey et al. [10] using PDPA. They reported that the droplet diameter in the combusting ethanol spray was reduced by 15% on the average by the acoustic oscillations. They have clarified that the decrease in the droplet diameter is mainly due to spray evaporation and not due to the

Presented as Paper 0502 at the 41st Aerospace Sciences Meeting and Exhibit, Reno, Nevada, 3–6 January 2003; received 14 November 2006; revision received 17 March 2008; accepted for publication 17 March 2008.

*Department of Aerospace Engineering; currently Department of Mechanical Engineering, University College London, Torrington Place, London WC1E 7JE, United Kingdom.

†Department of Aerospace Engineering; src@ae.iitm.ac.in.

effect of the acoustic oscillations on the atomization process for the kind of atomizer they have used. A similar atomizer is used in the present study.

Dutko et al. [11] studied the effects of resonant acoustic oscillations on the evaporation rate of a water spray within the resonating chamber of a pulse combustor burning natural gas. They reported that when resonant acoustic oscillations were present in the combustor, the evaporation rate was increased when compared with the steady-state combustion. The amount of water that was sprayed into the combustor and evaporated without wetting the walls and pooling of liquid water in the chamber was significantly increased by 25–30% [for a sound pressure level (SPL) of 168 dB] over the investigated range of conditions, when acoustic oscillations were excited in the combustor.

Although Gemmen et al. [6] and Sujith et al. [7] have showed substantial improvement in evaporation rates in the presence of strong acoustic oscillations, their works have been with single droplets. The studies with sprays, on the other hand, have not showed a similar level of enhancement in the evaporation rate with acoustics. The present work has been motivated by this apparent disparity.

The desire to evolve a compact device has necessitated multiple roles for the combustor, namely, to achieve complete combustion, to act as a resonant cavity, and to serve as a chamber to inject the spray for evaporation. It is well known that acoustic oscillations could be damped by spray droplets [12,13]. Besides, excitation of high-amplitude acoustic oscillations could enhance the heat loss to the walls, thereby making less heat available for evaporation of the spray. These contravening factors have required characterization of the acoustic field excited by the combustor developed in the present work and the heat losses under different conditions of acoustic excitation. These results, along with the effect of the acoustic oscillations on the spray evaporation rates are presented next, after the description of the experimental details. The mechanism of acoustic excitation in this combustor configuration is briefly discussed in the context of the past studies [2,14,15].

II. Experimental Details

A. Setup

The experimental setup used for this study is a laboratory-scale combustor for a maximum rating of 30 kW. Figure 1 shows a schematic of the experimental setup. It consists of a primary combustor, a water-spray injector segment, and a tailpipe.

The primary combustor is a 750-mm long stainless steel tube of 110-mm inner diameter. The inlet to the combustion chamber consists of two coaxial ducts, of which the outer duct allows air and the inner one allows fuel. Commercially available liquefied petroleum gas (LPG) is used as fuel in the present work. The airline is a 600-mm-long tube of 50 mm inner diameter. The air duct opens into the combustor through a divergent passage having a semicone angle of 45 deg. The fuel line is a tube 1800 mm in length, with an outer diameter of 19 mm. The fuel line terminates in a disk-shaped bluff body of 40-mm diameter, which helps in flame holding. The bluff body has 16 holes of 2-mm diameter each along the circumference

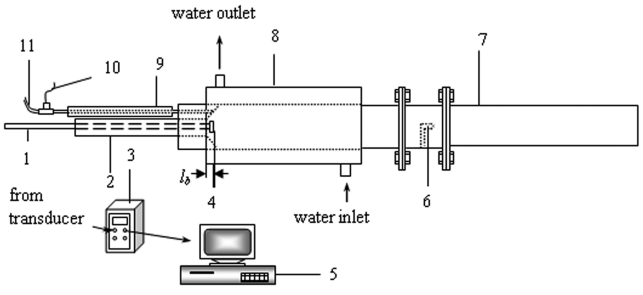

1. Fuel supply line, 2. Air supply line, 3. Signal amplifier, 4. Brass bluff body,
5. Computer, 6. Air blast nozzle, 7. Tailpipe, 8. Water cooling jacket,
9. Calibrated acoustic probe, 10. Transducer, 11. Semi-infinite tube.

Fig. 1 Schematic of the laboratory-scale bluff body combustor.

for fuel injection. The ability to move the bluff body in the axial direction along the divergent portion of the combustor enables the excitation of different modes of acoustic oscillations at different amplitudes in the combustor. The primary combustor is cooled by circulating water through a cooling jacket around it to mitigate its deformation due to thermal stresses.

Water is sprayed inside the combustion chamber using an air-blast atomizing system along the air flow direction. The spray nozzle is mounted in a short water-injector segment connected between the primary combustor and the tailpipe, all of which have the same inner diameter. The tailpipe is 900 mm long.

Acoustic decouplers are provided upstream of the air and fuel flows, between the flow measuring devices and the combustor, to decouple the measuring devices from the acoustic field inside the combustor. This is needed because the measurements made using rotameters are prone to errors of up to 15% due to the presence of a strong acoustic field [16]. The acoustic decouplers are over 3 times larger in diameter and over 5 times longer than the diameters of the respective inlet pipes to the combustor.

B. Measurements

Air is supplied to the combustor from a reservoir with a capacity of 30 m^3 at 1.3 MPa. The volume flow rate of air is measured using a venturimeter that is calibrated using a precalibrated rotameter in the range 300–1500 liters per minute (LPM) with an error of <2% of the full range. The volume flow rate of fuel is measured using an LPG rotameter (range 3–30 LPM, less than 2% error of the full range). The flow rate of water sprayed inside the combustor is determined by measuring the depression of the meniscus of a column of the water in a transparent reservoir and the time taken for the corresponding depression. The volumetric rate of water injection is calculated as $q_{\text{inj}} = (h \times A)/t$, where h is the depression of the meniscus, A is the area of cross-section of the graduated chamber, and t is the time taken for the depression of the meniscus. The flow rate of the cooling water is measured by noting the volume of water collected in a container during a given time interval. Chromel-alumel thermocouples are used to measure the temperature of the exhaust gases in the combustor and at the exit, the outside wall temperature, and the temperature of the cooling water at the inlet and the outlet.

The acoustic pressure oscillations in the combustor are measured at the divergent portion of the combustor inlet using a piezoelectric transducer (either Kistler Model 206 or PCB model 103A12, having sensitivities of 100 and 500 mV/psi, respectively). Data are acquired for 1 s at a sampling rate of 15,000 Hz, which is much higher than the expected dominant frequencies. This gives a bin size of 1 Hz for the fast Fourier transform (FFT) of the data.

To estimate the amount of water that exited the combustor in the form of droplets, that is, without undergoing evaporation, the Mie scattering technique is adopted. A thin light sheet from a He-Ne laser illuminates a region 3 mm away from the exit of the combustor tailpipe. The light scattered by the droplets is imaged using a high-sensitivity CCD camera.

C. Operational Conditions and Procedures

The ranges of variation of the different parameters in the study are given in Table 1. Because the goal of the present study is to examine the effect of self-excitation of a strong acoustic field on the water-spray evaporation rate, care has to be taken not to substantially alter the flow conditions between the situation when high-amplitude oscillations are excited and when they are not. The self-excitation of acoustic oscillations by the combustor is achieved primarily by adjusting the location of the bluff body relative to the combustor inlet, under a given set of flow conditions. The location of the bluff body is described by l_b as the distance between the inlet section of the divergent portion of the combustor and the downstream face of the bluff body. Preliminary tests have been performed in the range $0 < l_b < 125$ mm at specific air and fuel flow rates, but most subsequent tests are performed at two locations of the bluff body, that is, $l_{b1} = 12$ and $l_{b2} = 32$ mm, as indicated in Table 1. The variations in the air- and fuel-mass flow rates yield a corresponding variation in

Table 1 List of operating conditions

Parameter	Maximum value	Minimum value	Minimum step size	Other conditions
Bluff-body position l_b, mm	0	125	1	$\dot{m}_a = 13.1$ g/s $\phi = 0.47$
Air flow rate $\dot{m}_a$, g/s	9.4	22.5	1.9	$l_{b1} = 12$ mm $l_{b2} = 32$ mm
Fuel flow rate $\dot{m}_f$, g/s	0.27	1.15	0.04	$l_{b1} = 12$ mm $l_{b2} = 32$ mm

the overall fuel–air equivalence ratio ϕ in the range 0.18–1.86. The average air flow velocity at the combustor inlet (just downstream of the divergent section) is estimated from the flow-rate measurements as being in the range of 0.88–2.12 m/s.

In the experiments on water evaporation, the quantity of water exiting the combustor as droplets is quantified by calibration of their Mie scattering from a laser sheet at the exit of the combustor. The calibration is performed by spraying water inside the combustor at known flow rates in the range of 0.2–4.5 g/s under cold air flow conditions, without allowing for it to collect along the bottom of the combustor.

For relatively large quantities of water injected into the combustor under hot flow conditions, some amount of water gets collected along the bottom of the combustor wall. This process is referred to as *pooling* [11]. A part of the pooled water drains out of the combustor exit without undergoing evaporation. This is collected in a container for a specific duration, and its quantity is measured at the end of a run. As the combustor is not thermally insulated, the setup is allowed to attain thermal equilibrium over 15 min from the start of water spraying, before evaporation measurements are made.

III. Results and Discussion

A. Characterization of the Combustor

1. Acoustic Characteristics

The objective of this set of experiments is to determine the effect of the overall equivalence ratio and the air mass flow rate on the dominant frequency and pressure amplitude of the acoustic oscillations excited in the combustor developed in the present study. The acoustic amplitude could be varied by changing the bluff-body location l_b. A shift towards a higher acoustic mode occurs in the self-excitation of acoustic oscillations at high acoustic amplitudes, as the bluff body is moved towards the combustor to the location $l_b =$ 12 mm (l_{b1}), from higher values. Because the cross section of the inlet of the combustion chamber is divergent and the area of cross section reduces towards the inlet, movement of the bluff body towards the inlet in this region leads to an increase in local velocities. This may result in a higher frequency of vortex shedding, leading to mode shift from fundamental to the first harmonic. Yu et al. [15] have also reported similar sudden hopping of the dominant frequency when the inlet flow velocity is increased. The excitation of high-amplitude oscillations at the higher mode occurs over a wide range of overall equivalence ratio. The acoustic amplitude first increases and then decreases as the overall equivalence ratio is varied, as demonstrated by Sivasegaram and Whitelaw [14].

Attention is focused on the two bluff-body locations l_{b1} and l_{b2} to compare the variation of dominant frequency and acoustic pressure amplitude with the overall equivalence ratio, as these two locations are representative of excitation of relatively high and low levels of acoustic oscillations, respectively. Figure 2 shows these variations for the two preceding bluff-body locations over a wide range of air mass flow rates. Focusing first on Fig. 2a corresponding to l_{b1}, it can be seen that, as the equivalence ratio is increased in the fuel-lean side ($\phi < 1$), the dominant frequency shifts from a lower mode (referred to as mode A) to a higher mode (referred to as mode B), progressively, as the air flow rate is increased. The amplitude also correspondingly increases from the 500–1000 Pa range (∼148–154 dB) to about 2500–3500 Pa (∼162–165 dB and even higher under some conditions). As the conditions turn fuel rich, that is, when $\phi \geq 1$, the dominant frequency abruptly drops to another mode (referred to as mode C). There is a correspondingly drastic drop in the amplitude to less than 200 Pa. This latter jump is almost independent of the air mass flow rate, except at the lowest level tested. Mode A is around 80–90 Hz, and is identified as corresponding to the fundamental quarter-wave mode for the length of the combustor-tailpipe section, whereas mode B is around 230–260 Hz and is identified as its first harmonic. Mode C, being around 105–130 Hz, on the other hand, can be identified as the fundamental mode corresponding to the inlet duct with both ends closed. Note that these identifications are approximate and associated with the modes based on a quiescent mean-isothermal duct with idealized boundary conditions for purposes of qualitative understanding. The evaluation of the exact modes is complicated by the presence of mean flow, axial temperature gradients, distributed heat release and its acoustic

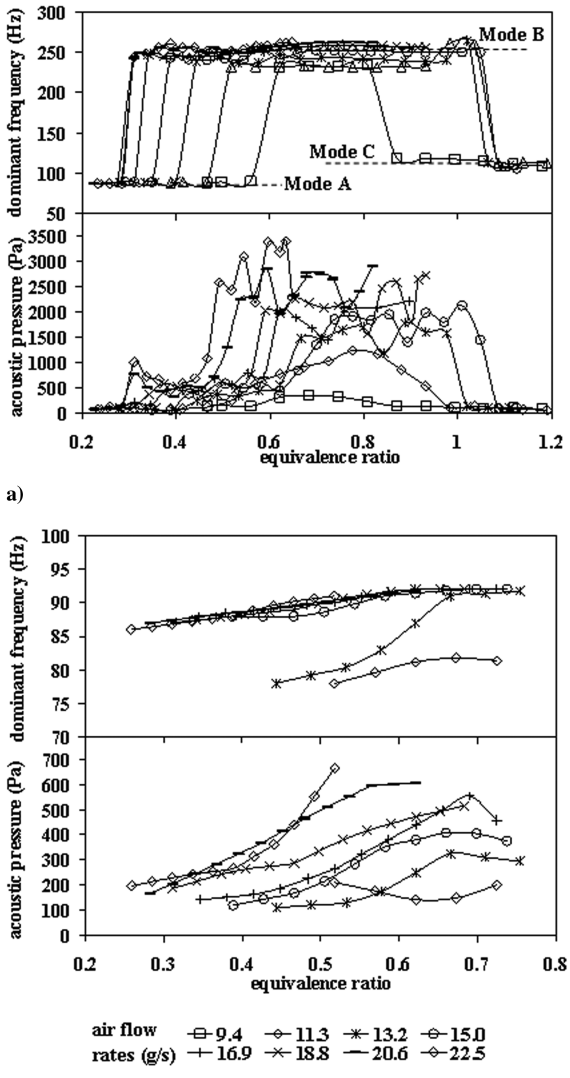

Fig. 2 Variation of dominant acoustic frequency and corresponding pressure amplitude with overall equivalence ratio for different air flow rates: a) $l_b = 12$ mm, b) $l_b = 32$ mm.

response, variations in the speed of sound, etc. During these experiments, it was observed that the l_b values for which maximum amplitude could be achieved were varied only by 1–2 mm for the different air flow and fuel flow rates tested. The excitation of the inlet duct's acoustic mode is a significant aspect of the work by Yu et al. [15], but it is observed only under some conditions in the present study at lower amplitude levels, as measured in the combustor. This is probably because the combustor length was maintained to be short relative to the inlet-duct length in that study, as opposed to the long combustor provided in the present study. Further, the presence of a nozzle in Yu et al. [15] offered the mechanism of vortex convection and impingement as providing a time scale and contributing to the instability period besides the acoustic time of the inlet-duct mode; this mechanism does not apply to the combustor with an open end as in the present study.

As opposed to the preceding information, the acoustic characteristics observed at l_{b2} shown in Fig. 2b indicate excitation of a relatively constant frequency of around 80–90 Hz (mode A) over the entire test range of the overall equivalence ratio for different values of the air mass flow rate. Correspondingly, the variations in the acoustic pressure amplitude do not show any jumps within the equivalence-ratio range tested and are generally in the 100–600 Pa (∼134–150 dB) range. An increase in the acoustic pressure amplitude with an increase in air mass flow rate and overall equivalence ratio is generally observed, which is due to increased levels of turbulent heat-release fluctuations.

2. *Flame Structure*

There is a significant and abrupt change in the flame structure corresponding to the transition from the relatively low-amplitude acoustic oscillations at the fundamental mode to high-amplitude oscillations at the first harmonic mode. Figure 3 shows the difference in the time-averaged appearance of the flame under these two conditions, when viewed from the combustor exit along its length. The flame zone is relatively very compact in the vicinity of the bluff body, is blue in color as with fuel-lean premixed flames, and exhibits apparently intense periodic oscillations, when the bluff body is located close to the inlet of the divergent portion of the combustor, that is, at l_{b1}. As opposed to this, it is elongated along most of the combustor length and is yellowish–orange in color, typical of a diffusion flame when the bluff body is located away from the inlet of the divergent portion of the combustor, that is, at l_{b2}. As a result, a compact heat-release zone prevails when strong acoustic oscillations are self-excited, whereas a distributed heat-release zone prevails when the acoustic oscillations are self-excited at low-pressure-amplitude levels. Such a drastic change in the flame structure has also been reported by other investigators in the past, such as Schadow [17]. This has important implications on the effect of acoustic oscillations on heat transfer of the combustor in terms of temperature distribution in the flame zone, as can be seen in the following subsections.

Unlike almost all of the previous investigations, such as Sivasegaram and Whitelaw [14], Yu et al. [15], and Schadow and Gutmark [2], which were on premixed combustors, the present study adopts what is nominally a nonpremixed combustor, with the fuel being injected at the periphery of the bluff body used to stabilize the flame, that is, the fuel is injected just upstream of the flame zone. Therefore, acoustic enhancement of fuel–air mixing is an important step in the combustion and chemical heat-release process, whose fluctuations drive the acoustic oscillations, in turn.

Another aspect to note in this geometry is the possibility of impinging shear-layer instability due to flow separation and vortex roll-up at the inlet to the divergent section and the impingement of the vortical structures at the upstream corner of the bluff body [18]. This is further influenced from upstream by the oscillations in the inlet duct, which, in turn, are coupled with the oscillations in the combustor where the acoustic driving occurs due to the flame fluctuations there. This is a complex set of processes that requires further investigation, but it has not been pursued in this study because the focus is on the efficacy of the excited acoustic oscillations to enhance the evaporation rate of a water spray.

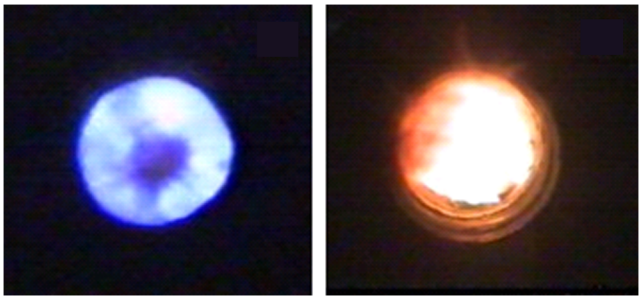

a) b)

Fig. 3 Images of the luminous flame viewed along the length of the combustor from the exit with the bluff body at two locations: a) l_{b1} and b) l_{b2}, corresponding to self-excitation of high- and low-amplitude acoustic oscillations, respectively.

A third mechanism in operation in the present situation with regard to the excitation of oscillations is the possibility of equivalence-ratio fluctuations, because the fuel injection is within the acoustic field of the duct and, therefore, could fluctuate [5]. In general, this mechanism would coexist with that due to the heat-release-rate fluctuations from the flame in response to the prevalent oscillations and due to vortex shedding.

It is important to note from Fig. 3 that the combined effect of these mechanisms is not only to cause heat-release fluctuations but also to change the mean structure of the flame itself, under self-excited conditions.

3. *Heat-Transfer Characteristics*

The coupling between the acoustic oscillations and the flame zone in the combustor developed in the present work, as observed in the preceding subsections, leads to enhanced heat transfer to the water-cooling jacket around the combustor and from the tailpipe to the ambient. The heat transfer from the combustor and tailpipe walls has implications on the rate of spray evaporation. This aspect has been studied as part of the present work.

It is well known that the excitation of high-amplitude acoustic oscillations causes wall heat transfer in general. This is compounded by the compactness of the flame zone under conditions of high-amplitude acoustic excitation, which results in an early increase in the mean temperature along the length of the combustor, thereby increasing heat transfer to the surrounding water-cooling jacket and in the tailpipe further. As a result, the mean temperature of the exhaust products is lower when strong acoustic oscillations are excited than otherwise, leading to apparently counterintuitive observations. Figure 4 shows variations of the exhaust gas

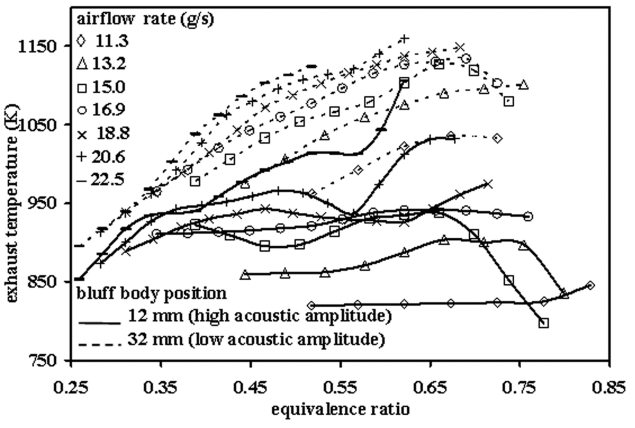

Fig. 4 Variation of exhaust gas temperature along the centerline with the overall equivalence ratio in the presence and absence of high-amplitude acoustic excitation at different air flow rates.

temperature measured at the combustor centerline as a function of the equivalence ratio at different air flow rates and along the radius for one set of operating conditions in the presence and absence of high-amplitude acoustic oscillations corresponding to the two bluff-body locations l_{b1} and l_{b2}, respectively. It can be seen that the exhaust temperature is lower in the presence of high-amplitude acoustic oscillations under all conditions tested, although this condition is accompanied by intense mixing of the reactants and high combustion intensity. This is because of increased heat loss to the walls of the combustor in the presence of strong acoustic oscillations.

First, the heat loss to the water-cooled portion of the combustor is considered. The fractional heat loss due to water cooling is given by

$$\eta_{\mathrm{HL}} = \frac{Q_{\mathrm{water}}}{Q_{\mathrm{input}}} \tag{1}$$

where Q_{water} is the heat loss due to water cooling, and Q_{input} is the heat input in the form of fuel addition and combustion in the combustor. Q_{water} is given by

$$Q_{\mathrm{water}} = \dot{m}_{\mathrm{water}} C_w (T_{\mathrm{in}} - T_{\mathrm{out}}) \tag{2a}$$

where $\dot{m}_{\mathrm{water}}$ is the mass flow rate of the cooling water, C_w is the specific heat capacity of water, and T_{in} and T_{out} are the temperature of the water at the inlet and outlet of the water-cooling jacket. The mass flow rate and the temperatures are measured quantities in the present work, as mentioned earlier. Q_{input}, on the other hand, is given by

$$Q_{\mathrm{input}} = \dot{m}_f \Delta h_f \tag{2b}$$

where Δh_f is the heating value of the fuel (taken as 44 MJ/kg for LPG). Figure 5 shows the variation of fractional heat loss with the overall equivalence ratio for the bluff body at l_{b1} and l_{b2} for an air flow rate of 15.016 g/s. The acoustic-pressure amplitude variations under these conditions are shown in the same figure for correlation with the heat loss. Note that the fractional heat loss is substantial, mainly as a result of the water-cooling. However, this has been necessitated to ensure the structural integrity of the combustor walls during continuous operation over a long duration. The figure shows a strong correlation in the trend between the fractional heat loss and the acoustic-pressure amplitude variations with the overall equivalence ratio. For l_{b2}, both quantities are nearly constant and at relatively low levels. But, for l_{b1}, the fractional heat loss and the acoustic pressure amplitude first increase sharply at about the equivalence ratio of 0.5, maintain a high value, and then fall sharply at around the equivalence ratio of 0.92. It is interesting that the fractional heat loss outside the preceding equivalence-ratio range is nearly the same as that for l_{b2}. This clearly shows that the sound pressure levels significantly affect the heat losses; that is, with an increase in the sound pressure levels the heat losses increase.

Next, we consider the heat transfer in the tailpipe. The convective heat-transfer coefficient in the tailpipe has also been calculated from the temperature measurements, using the following relation [19]:

$$h = \frac{\dot{m}_p C_p}{\pi D l_T} \ell_n \left[\frac{T_1 - T_a}{T_2 - T_a} \right] \tag{3}$$

Here, $\dot{m}_p$ is the mass flow rate of the combustion products, C_p is their specific heat capacity at constant pressure, D is the diameter of the combustor duct, l_T is the distance between two temperature measurement locations along the tailpipe, T_1 and T_2 are the temperatures measured at the two locations, and T_a is the ambient temperature. In the present work, temperatures are measured at 250 mm and 950 mm upstream of the combustor exit, both locations being downstream of the water-cooled portion. Figure 6 shows the heat-transfer coefficient as a function of the rms pressure amplitude observed in the combustor at two different air flow rates. These different pressure levels are obtained by adjusting the bluff-body location, and they are reported in terms of rms values to account for disparities in the dominant frequencies over the observed range. It can be seen from the preceding figure that the heat-transfer coefficient in the tailpipe also systematically increases with the acoustic pressure in the combustor, as in the case with the water-cooled portion.

4. *Summary of Combustor Characteristics*

Summarizing the characterization of the combustor for the spray evaporation studies next, it can be seen that movement of the bluff body closer to the combustor inlet leads to excitation of high-amplitude oscillations at the first harmonic with the bluff-body end acting like an acoustically closed end. For farther location of the bluff body, the fundamental quarter-wave mode is excited at relatively low amplitudes. At the high-amplitude conditions, the flame is compact and held close to the bluff body; it appears to be like a premixed flame. At low-amplitude conditions, the flame is distributed over a large length of the combustor and is orange in color, more like a diffusion flame. This shows that the acoustic oscillations influence the mixing of the fuel and air that burn to excite the oscillations, in turn. The heat transfer to the water-cooled portion and the tailpipe is larger with high-amplitude oscillations than otherwise. This is because the temperature increases rapidly across a compact flame, and there is more heat to be lost to the combustor walls subsequently downstream in the case of high-amplitude acoustic excitation than in the other case; wherein a distributed combustion process increases the temperature more gradually, probably to lower maximum levels before heat is lost to the walls of the combustor further downstream to a lesser extent. Ultimately, the exit temperature is higher in the latter case than in the former. These processes are qualitatively depicted schematically in Fig. 7.

B. Water-Spray Evaporation Studies

The spray nozzle is located near the acoustic velocity antinode of the first harmonic in the present study, because it is expected to significantly enhance heat/mass transfer, as established by Matta et al. [20]. Using the calibration of the Mie scattering intensity with

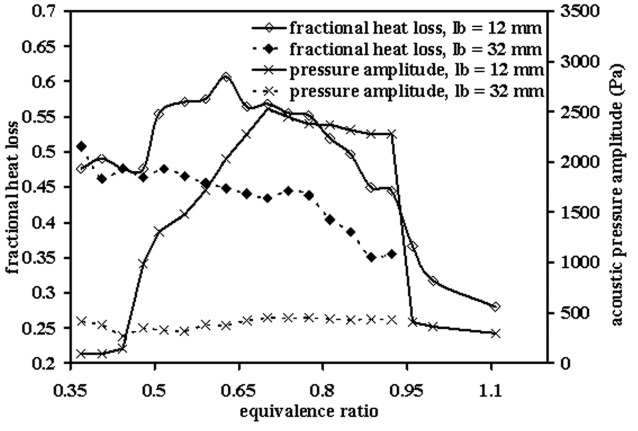

Fig. 5 Effect of acoustic pressure amplitude on the fractional heat loss to water cooling at the walls of the combustor; air flow rate = 15.0 g/s.

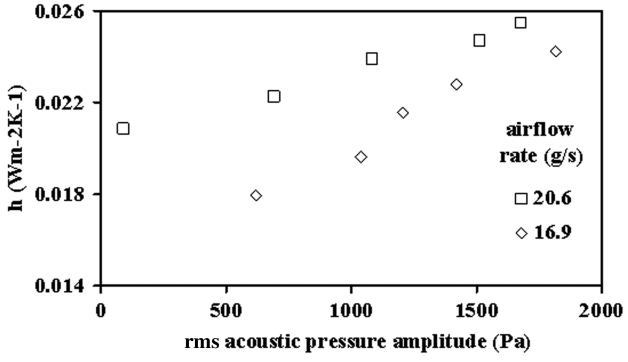

Fig. 6 Variation of convective heat-transfer coefficient h in the tailpipe with the acoustic pressure amplitude at different air flow rates.

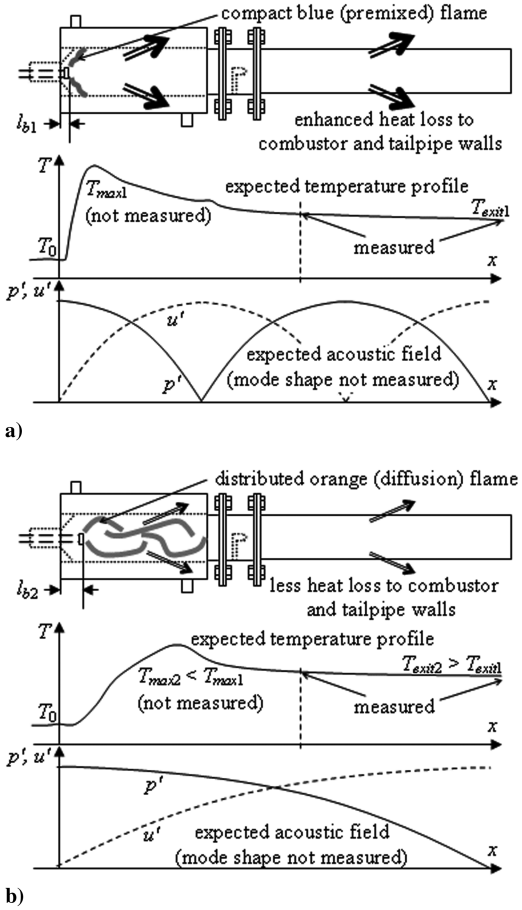

Fig. 7 Schematic qualitative depiction of processes in the combustor under conditions of excitation of oscillations of a) high amplitude and b) low amplitude.

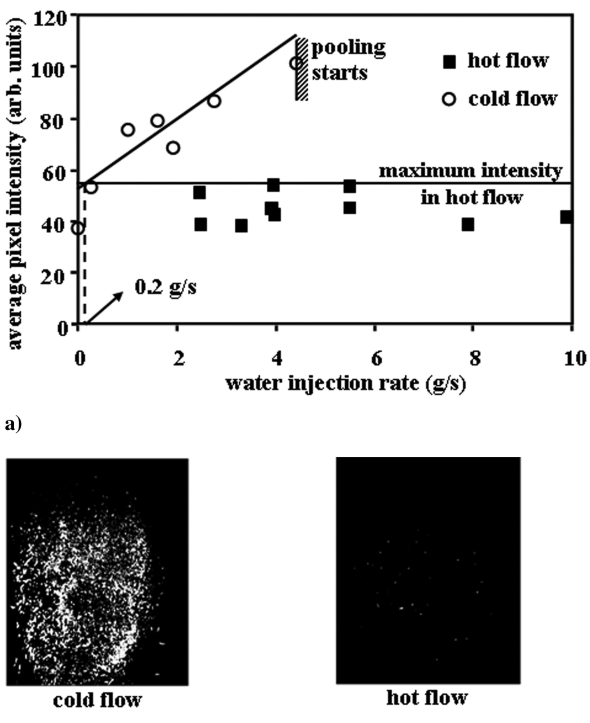

Fig. 8 Calibration to quantify water exiting the combustor in the form of droplets: a) variation of average pixel intensity of Mie scattering of water droplets and b) typical Mie scattering images under cold and hot flow conditions, exiting the combustor.

the quantity of water injected under cold flow conditions, it was found that a maximum of 0.2 g/s of water exited the combustor under hot flow conditions regardless of the level of acoustic excitation, even for the maximum water injection rate tested (15 g/s). Figure 8 shows the average pixel intensity (API) of Mie scattering as the amount of water injected is increased under cold and hot flow conditions. Typical images of Mie scattering by water-spray droplets exiting the combustor under cold and hot flow conditions for the same rate of injection of water into the combustor are also shown in Fig. 8. It can be seen clearly that the average pixel intensity of the light scattered from the droplets is negligible because of evaporation under hot flow conditions when compared with the case without any evaporation under cold flow conditions. Correspondingly, the amount of water droplets exiting the combustor in suspended form, that is, less than 0.2 g/s, is considered to be negligible.

The evaporation of water injected inside the combustor is due to evaporation of both the suspended water spray and the pooled water. The water evaporation rate is determined as

$$\dot{m}_{\text{evap}} = \dot{m}_{\text{inj}} - \dot{m}_{\text{coll}} \tag{4}$$

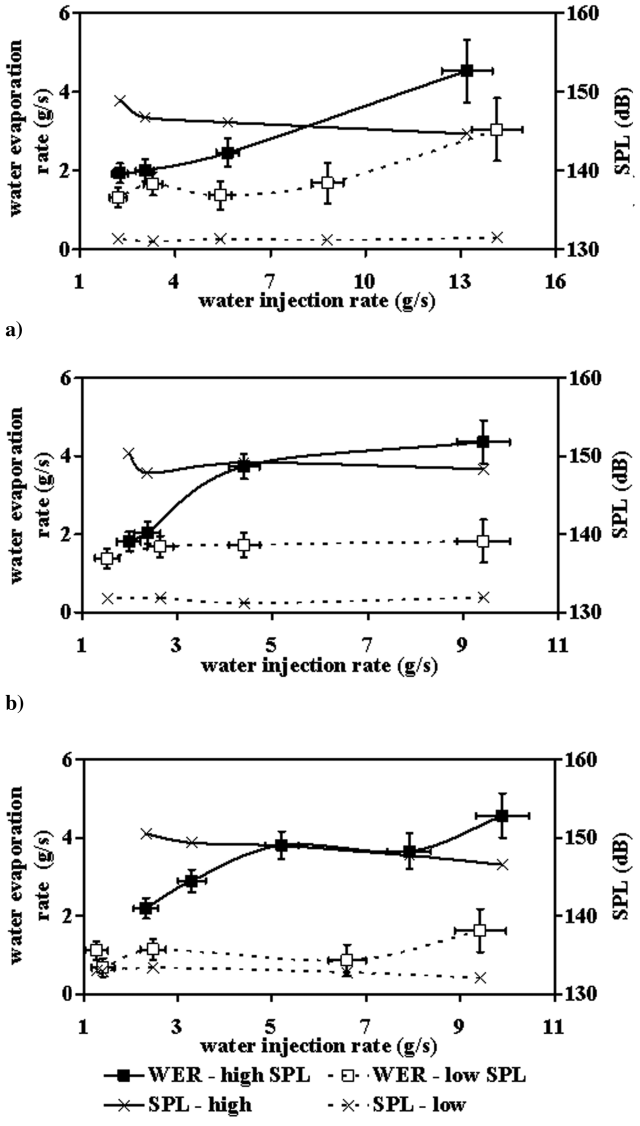

Fig. 9 Variation of water evaporation rate with the water injection rate at different air flow rates: a) 16.8, b) 20.6, and c) 22.5 g/s. The fuel flow rate is 0.53 g/s. The corresponding equivalence ratios are 0.48, 0.40, and 0.36. The excited sound pressure levels are shown alongside for correlation.

where $\dot{m}_{inj}$ is the mass flow rate of water injected and $\dot{m}_{coll}$ is the mass of water collected at the exit of the combustor per unit time. The uncertainty in the estimation of $\dot{m}_{evap}$ is calculated by incorporating the measurement errors.

Figure 9 shows the variation of water evaporation rate with the rate of water injection under conditions of both high- and low-amplitude acoustic excitation, for air flow rates of 16.8, 20.6, and 22.5 g/s. The fuel flow rate is maintained at 0.53 g/s in these experiments. The variations in the excited levels of acoustic pressure amplitude under these operating conditions are shown alongside for correlation. Note that the difference in the sound pressure levels between the two conditions of high- and low-amplitude excitation is ~12–15 dB similar to that observed earlier without water spraying, which is still substantial despite the presence of water spray in these experiments. It can be clearly seen that the water evaporates at a considerably greater rate under conditions of high acoustic pressure amplitudes than otherwise (~100% increase in some cases). The increase in the water evaporation rate with acoustic pressure amplitude is more with a greater amount of water injection, although the error in the $\dot{m}_{evap}$ measurement also increases. Evidently, the evaporation enhancement level is off for high values of $\dot{m}_{inj}$. Figure 9 also indicates that the dependence of the enhancement in the water evaporation rate on the air flow rate due to the acoustic oscillations is nonmonotonic.

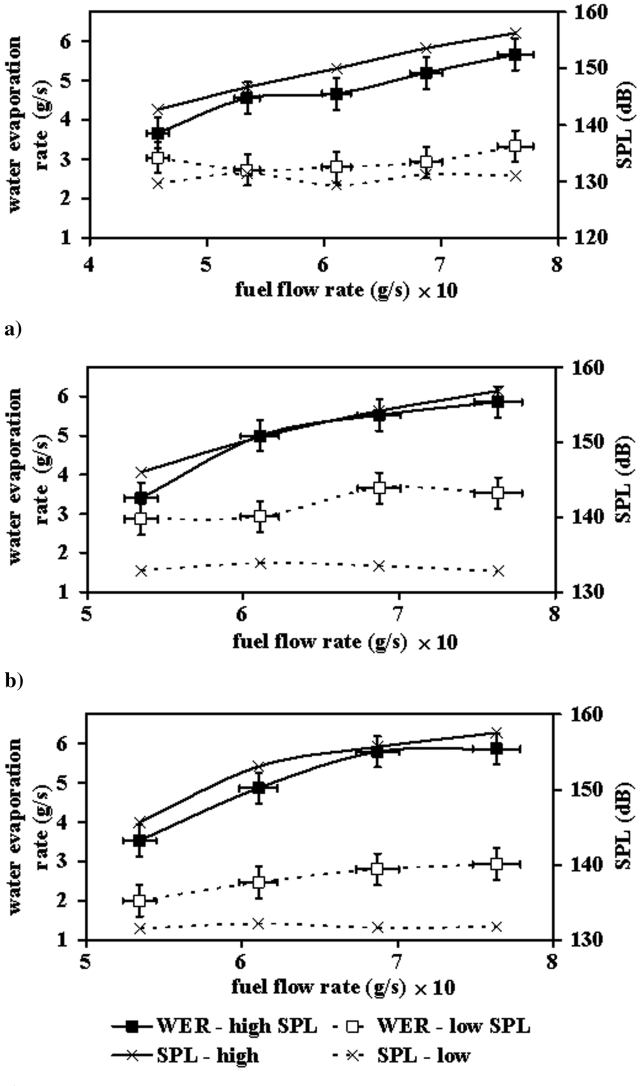

Fig. 10 Variation of water evaporation rate with the fuel flow rate at different air flow rates: a) 16.8 ($\phi \sim 0.47$–0.73), b) 20.6 ($\phi \sim 0.37$–0.60), and c) 22.5 g/s ($\phi \sim 0.34$–0.54). The water injection rate is 6.6 g/s. The excited sound pressure levels are shown alongside for correlation.

The water-spray evaporation is not only dependent on the heat-transfer rates to the droplets but also on the heat available for evaporation. The heat available in the combustor for evaporation of the water spray is adjusted by the rate of fuel flow into the combustor. Figure 10 shows the variation of the water evaporation rate with the fuel flow rate under high and low SPL conditions, for the same air flow rates as mentioned earlier, with the water injection rate maintained at 6.6 g/s in all these cases. As expected, the water evaporation rate increases with increase in the fuel addition, but levels off for sufficiently large values of the fuel flow rate, particularly at lower equivalence ratios, regardless of high or low SPL. However, the enhancement in water evaporation rate is seen to occur uniformly over the entire range of fuel flow rates tested.

Further experiments have been conducted to determine the dependence of water evaporation rates on acoustic pressure amplitudes, by varying the bluff-body location, for given air and fuel flow rates and water injection rate. These experiments are performed at two air flow rates, namely 18.8 and 20.6 g/s. The fuel flow rate and the water injection rate are maintained at 0.53 and 6.6 g/s respectively. Figure 11 shows the plot of the water evaporation rate (WER), normalized as $(\mathrm{WER}/\dot{m}_a)/(p'_{rms}/p_0)$, vs the normalized rms acoustic velocity amplitude $u'_{rms}/\bar{u}$ (estimated as $\sim p'_{rms}/\rho_0 c\bar{u}$) excited in the combustor. Here, $\dot{m}_a$ is the air mass flow rate, p'_{rms} is the rms acoustic pressure amplitude measured in the combustor, p_0 is the mean ambient pressure (taken as 10^5 Pa), ρ_0 is the mean air flow density at the combustor inlet, c is the reference speed of sound taken as 634 m/s corresponding to a typical spatially averaged time-mean temperature of 1000 K in the combustor, and $\bar{u}$ is the spatio-temporal average air flow velocity at the combustor inlet. The WER is nondimensionally represented as mentioned earlier because the water evaporation is expected to increase with both air convection and the acoustic oscillations. It is seen in Fig. 11 that the data obtained at the two different air flow rates fairly overlap over each other for the choice of the dimensionless groups adopted, suggesting that 1) increase in the convective effect only partly increases the water evaporation but is substantially influenced by the amplitude of acoustic oscillations prevalent in the combustor and 2) the normalized acoustic velocity is the appropriate quantity that affects the vaporization process, as indicated by Sujith et al. [8]. It is also seen from the figure that there exists a threshold value of acoustic pressure amplitude at each air flow rate, above which the water evaporation is significantly enhanced. This is also in conformation with the theoretical prediction on single droplets by Sujith et al. [8] that, with increase in acoustic velocity, the evaporation rate would decrease until it reaches a minimum, beyond which it would increase.

It can also be deduced from Fig. 11 that the threshold amplitude increases with an increase in air flow rate. Significant heat transfer to and mass transfer from the spray droplets occurs in the presence of acoustic oscillations only when the oscillations are strong enough to cause flow reversal during each cycle [21]. This drastically increases the rates of transport processes, besides increasing the residence times of the spray droplets. At a higher mean flow rate of air, it takes greater acoustic velocity amplitude to cause this process. Because the acoustic velocity amplitude is proportional to the sound pressure level, the threshold pressure amplitude is observed to increase with increase in the air flow rate.

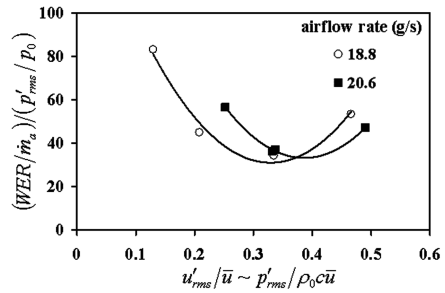

Fig. 11 Normalized WER as a function of normalized estimated rms acoustic-velocity amplitude. The fuel flow rate and water injection rate are 0.53 ($\phi = 0.43$ and 0.40) and 6.6 g/s, respectively.

IV. Conclusions

A laboratory-scale self-excited bluff-body combustor is developed. The ability of the combustor to excite a wide range of SPLs by adjusting the bluff-body location from 134 dB to as high as 165 dB has been demonstrated for a wide range of mass flow rates of air and fuel. Excitation of high-amplitude oscillations is accompanied by a shift in the mode from the fundamental to the first harmonic, at different equivalence ratios depending upon the air flow rate. The flame structure appears to transition from an elongated diffusion flame to a compact premixed flame as the SPL grows from low to high values.

The presence of strong acoustic oscillations is found to increase the rate of water-spray evaporation, despite increased heat losses to the combustor walls (up to 40% increase for increase in the SPL from 145 to 160 dB). The water evaporation rate is enhanced by as high as 107% for a sound pressure level of 156 dB. The results indicate that there exists a threshold amplitude level above which the enhancement of the water evaporation rate is significant. These results are very promising for application in various commercial and practical applications such as spray drying, calcining, incineration, etc.

Acknowledgments

This research was funded by a grant from the Ministry of Human Resources Development, Government of India, under the Thrust Areas in Technical Education Scheme. The authors would like to thank Jayanti Srinivas for his constructive criticisms and interest in this work, and the anonymous reviewer who prompted the non-dimensionalization of the final results.

References

[1] Kan, T., Matta, L. M., Jagoda, J. I., and Zinn, B. T., "Acoustic Enhancement of the Combustion of Solids in High Reynolds Number Flows," AIAA Paper 99-0345, 1999.

[2] Schadow, K. C., and Gutmark, E. J., "Combustion Instability Related to Vortex Shedding in Dump Combustors and their Passive Control," *Progress in Energy and Combustion Science*, Vol. 18, 1992, pp. 117–132.
doi:10.1016/0360-1285(92)90020-2

[3] Rayleigh, J. W. S., *Theory of Sound*, Dover, New York, 1945.

[4] Gutmark, E. J., Schadow, K. C., Sivasegaram, S., and Whitelaw, J. H., "Interaction Between Fluid-Dynamic and Acoustic Instabilities in Combusting Flows Within Ducts," *Combustion Science and Technology*, Vol. 79, 1991, pp. 161–166.
doi:10.1080/00102209108951763

[5] Lieuwen, T. C., Torres, H., Johnson, C., and Zinn, B. T., "A Mechanism of Combustion Instability in Lean Premixed Gas Turbine Combustors," *Journal of Engineering for Gas Turbines and Power*, Vol. 123, No. 1, 2001, pp. 182–190.
doi:10.1115/1.1339002

[6] Gemmen, R. S., Keller, J. O., and Arpaci, V. S., "Pulse Combustion: Numerical Analysis of Droplet Mass Transfer Enhancement," *Thermo-Physical Aspects of Energy Conversion: Transactions of the American Society of Mechanical Engineers*, Vol. 16, American Society of Mechanical Engineers, Fairfield, NJ, 1990, pp. 81–90.

[7] Sujith, R. I., Waldherr, G. A., Jagoda, J. I., and Zinn, B. T., "Experimental Investigation of the Evaporation of Droplets in Axial Acoustic Fields," *Journal of Propulsion and Power*, Vol. 16, No. 2, 2000, pp. 278–285.

[8] Sujith, R. I., Waldherr, G. A., Jagoda, J. I., and Zinn, B. T., "A Theoretical Investigation of the Behavior of Droplets in Axial Acoustic Fields," *Journal of Vibration and Acoustics*, Vol. 121, 1999, pp. 286–294.
doi:10.1115/1.2893978

[9] McQuay, M. Q., and Dubey, R. K., "The Interaction of Well-Characterized Longitudinal Acoustic Waves with a Non-Reacting Spray," *Atomization and Sprays*, Vol. 8, 1998, pp. 419–437.

[10] Dubey, R. K., Black, D. L., McQuay, M. Q., and Carvalho, J. A., Jr., "The Effect of Acoustics on an Ethanol Spray Flame in a Propane-Fired Pulse Combustor," *Combustion and Flame*, Vol. 110, 1997, pp. 25–38.
doi:10.1016/S0010-2180(97)00061-8

[11] Dutko, A. C., Matta, L. M., Scarborough, D. E., and Zinn, B. T., "Acoustic Enhancement of Water Spray Evaporation Within a Pulse Combustor," AIAA Paper 2000-0595, 2000.

[12] Marble, F. E., and Candel, S. M., "Acoustic Attenuation in Fans and Ducts by Vaporization of Liquid Droplets," *AIAA Journal*, Vol. 13, No. 5, 1975, pp. 634–639.
doi:10.2514/3.49777

[13] Lyman, F. A., "Attenuation of High-Intensity Sound in a Droplet Laden Gas," *Journal of Sound and Vibration*, Vol. 51, 1977, pp. 219–235.
doi:10.1016/S0022-460X(77)80033-3

[14] Sivasegaram, S., and Whitelaw, J. H., "Oscillations in Axisymmetric Dump Combustors," *Combustion Science and Technology*, Vol. 52, 1987, pp. 413–426.
doi:10.1080/00102208708952586

[15] Yu, K. H., Trouve, A., and Daily, J. W., "Low-Frequency Pressure Oscillations in a Model Ramjet Combustor," *Journal of Fluid Mechanics*, Vol. 232, 1991, pp. 47–72.
doi:10.1017/S0022112091003622

[16] Diederichsen, J., "A Singing Flame as a Tool for Evaluation of Damping Agents for Solid Propellant Rocket Motors," *Combustion and Flame*, Vol. 7, 1963, pp. 29–37.

[17] Schadow, K. C., "Active Combustion Control for Propulsion Systems," *AFOSR Workshop on Dynamics and Control of Combustion Instabilities in Propulsion and Power Systems*, California Inst. of Technology, Pasadena, CA, 20–22 Nov. 1997.

[18] Rockwell, D., "Oscillations of Impinging Shear Layers," *AIAA Journal*, Vol. 21, No. 5, 1983, pp. 645–663.
doi:10.2514/3.8130

[19] Munjal, M. L., *Acoustics of Ducts and Mufflers*, Wiley, New York, 1987.

[20] Matta, L. M., Zinn, B. T., and Jagoda, J. I., "Experimental Study of Acoustic Velocity Effects on Simulated Solid Fuel Pyrolysis," *AIAA Journal*, Vol. 35, 1997, pp. 1493–1498.

[21] Drummond, C. K., "Mass Transfer from a Naphthalene Sphere Under Oscillatory Flow," M.S. Thesis, Mechanical Engineering, Syracuse Univ., Syracuse, NY, 1979.

T. Lieuwen
Associate Editor